

RESEARCH PAPER

Radar micro-Doppler mini-UAV classification using spectrograms and cepstrograms

RONNY I.A. HARMANNY¹, JACCO J.M. DE WIT² AND GILLES PREMEL-CABIC¹

The radar micro-Doppler signature of a target is determined by parts of the target moving or rotating in addition to the main body motion. The relative motion of these parts is characteristic for different classes of targets, e.g. the flapping motion of a bird's wings versus the spinning of propeller blades. In the present study, the micro-Doppler signature is exploited to discriminate birds and small unmanned aerial vehicles (UAVs). Emphasis is on micro-Doppler features that can be extracted from spectrograms and cepstrograms, enabling the human eye or indeed automatic classification algorithms to make a quick distinction between man-made objects and bio-life. In addition, in case of man-made objects, it is desired to further characterize the type of mini-UAV to aid the threat assessment. Also this characterization is done on the basis of micro-Doppler features.

Keywords: Radar signal processing and system modeling, Radar applications

Received 31 October 2014; Revised 1 May 2015; Accepted 5 May 2015; first published online 8 June 2015

I. INTRODUCTION

Within the security and defense domain, radar is more and more applied in the confined and crowded urban and littoral environments. Consequently, there is a demand for detecting and classifying a wider range of small targets such as mopeds, dismounts, animals, birds, flocks of birds, and mini-drones. Basically, detection of these smaller targets requires lowering the detection threshold, with respect to both target radar cross section (RCS) and Doppler velocity. However, the sheer number of objects in crowded littoral and urban environments may potentially saturate the radar signal processing, leading to, e.g. lost tracks. Ultimately, situational awareness is affected.

In these environments, full situational awareness can be maintained only if target classification can be done reliably and rapidly. Rapid classification allows filtering-out objects that are irrelevant for the current mission. For this first rapid classification, distinction between broad target classes may be sufficient. Depending on the mission, these broad classes could be *man-made object*, i.e. a potential threat, and *bio-life*, i.e. a non-threat, such as a bird. In a next classification step, it is desired to provide further separation within the potential threat classes to aid the threat assessment. For instance, the size or number of rotors of a drone may be an indication of its maximum payload. In this paper, the

potential of exploiting micro-Doppler properties for this two-step classification approach will be reviewed.

The classification problem addressed within the current study focuses on recognizing small unmanned aerial vehicles (UAVs). Mini-UAVs are an emerging threat and exhibit so-called “LSS” characteristics, for Low (altitude), Small (RCS), and Slow (speed), which makes them challenging radar targets when they operate in an environment with for instance birds.

To reduce the number of false alarms, it is important to quickly classify a UAV as a man-made object, preferable before the tracking stage where the identity of all objects currently present is maintained, and thus the number of irrelevant objects should be minimal to prevent track overload. In the next step, further characterization of the UAV is desired. Some characteristics of interest are the type of UAV, the number of rotors, approximate size, etc. This classification can be done by a trained human operator just by visual inspection of the pre-processed measurement data. It is also possible to use automatic recognition. Key is that the data are measured and presented such that certain features can be extracted that, combined, characterize the target class. For instance, a simple maximum a posteriori probability (MAP) classifier can be used to perform automatic classification. An important advantage of this approach is that this type of classifier also works with a subset of available features, in case some features are unstable or of low quality.

In the study presented here, the emphasis is on micro-Doppler features that enable fast distinction between birds and mini-UAVs and that can be derived from spectrograms and cepstrograms in a rather straightforward manner. The features represent actual physical properties of the target and the proposed method allows defining a classifier

¹Thales Nederland B.V., Sensors, Advanced Development, Delft, The Netherlands.
Phone: +31 15 251 78 29

²TNO, Department of Radar Technology, The Hague, The Netherlands

Corresponding author:

R.I.A. Harmanny

Email: ronny.harmanny@nl.thalesgroup.com

without the need to construct target models based on training sets. Some explanatory examples of spectrograms of real and synthetic targets, both man-made objects and bio-life, can be found in [1]. This work is also a good starting point for understanding the micro-Doppler phenomenon in general, feature extraction and related micro-Doppler concepts.

The generation of spectrograms and cepstrograms is discussed in Sections II and III. In Section IV, examples are shown of spectrograms and cepstrograms from actually measured data. Relevant features for classification are identified in Section V. Section VI discusses an implementation of feature extraction and classification, and some results of these are shown in Section VII. Finally, some conclusions are presented in Section VIII.

II. SPECTROGRAM GENERATION

A spectrogram is a two-dimensional (2D)-graphical “waterfall” representation of the spectral content of a signal as function of time, where the power level in each time–frequency cell is taken from a color or gray scale. The appearance of a spectrogram depends on waveform and processing parameters, which will be discussed next.

A spectrogram is obtained by taking the magnitude squared of the short-time Fourier transform (STFT) of a discrete signal, where the STFT can be written as:

$$\begin{aligned} \text{STFT}\{x[n]\} &\equiv X(m, k) \\ &= \sum_{n=-\infty}^{\infty} x[n]w[n-m]e^{-j2\pi kn/N}. \end{aligned} \quad (1)$$

Here, $x[n]$ is the discrete signal, $w[n]$ is the discrete window function, which is non-zero in $[0..N]$ and zero elsewhere, n is the sample number, N is the number of samples in the analysis window, and k is an index for the frequency $k\omega_0$, where $\omega_0 = 2\pi f_s/N$ with sample rate f_s . For radars measuring range and Doppler, f_s in this paper is sometimes referred to as pulse repetition frequency (PRF) in case of pulse radars and sweep repetition frequency (SRF) in case of frequency-modulated continuous-wave (FMCW) radars. Index m determines the position of the analysis window. By repeatedly calculating the STFT with increasing m using a certain step size Δm , the spectrogram can be obtained. The step size Δm can be chosen such that a certain overlap between two consecutive analysis windows is realized, which gives a smoother result in the time dimension. Each calculation of the STFT gives a single column in the spectrogram, which will be referred to as a “trace”.

If we want to generate a visually useful spectrogram of a certain event, such as the flapping of a bird’s wing, then we need to choose an appropriate value for N . As a rule of thumb, we should choose to have the integration interval N/f_s as a fraction of the length of the event. This we refer to as the “short integration interval”. The wing beat period of the majority of bird species in steady flight is in the range of 0.05–0.5 s [2]. By assuming a moderate wing beat period of 0.1 s, the suitable integration interval to capture the details of a single wing beat cycle is of the order of 20 ms. The maximum radial velocity associated with flapping wings is about 15 m/s depending on the aspect angle. Consequently,

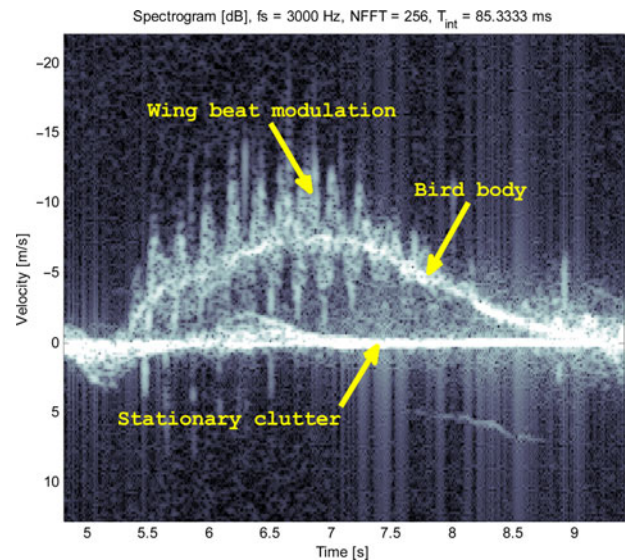


Fig. 1. Measured spectrogram of a bateleur (*Terathopus ecaudatus*)

the required sample rate f_s is relatively low, i.e. several kilohertz in X-band. A spectrogram of a flying bird, measured with an X-band continuous-wave (CW) radar, is shown in Fig. 1. For different bird species the spectrogram will appear different, e.g. in terms of wing beat frequency and amplitude, but comparable in terms of wing beat modulation around the (usually stronger) body echo.

Compared with flapping wings, spinning rotor blades constitute much faster events with much higher associated velocities. The rotor rotation period of mini-UAVs is of the order of milliseconds with related blade tip velocities of perhaps 200 m/s or even higher. The required sample rate f_s is therefore very high, of the order of tens of kilohertz. With a CW radar, such high sample rates are achievable, as well as with some short-range surveillance radars. Considering typical medium and long-range surveillance radars, however, such a high sample rate is unfeasible.

For periodic events that are stable to some extent, such as the spinning of rotor blades, “long integration intervals” can be applied for generating the spectrogram. By applying longer integration time, several revolutions of the rotor blades are included. The instantaneous spectral content is now dominated by the rotation rate of the blades causing modulation peaks. The instantaneous radial velocity of the blade tips is no longer observable. The difference between short and long integration interval is clearly visible in the measured spectrograms shown in Fig. 3 (top left and right). In case of long integration time, under sampling (i.e. lower sample rates) can be allowed if “cepstral analysis” is applied, as will be discussed in the next section.

III. CEPSTROGRAM GENERATION

Cepstral analysis can be used to assess the rate of change in a spectrum and it has been used for, e.g. characterizing seismic echoes from earth quakes and for human speech analysis. Cepstral analysis is based on the power cepstrum, which is defined as the power of the inverse Fourier transform of the logarithm of the power spectrum [3]. Congruently to the

STFT and spectrogram, a short-time cepstrum [4] and “cepstrogram” have been proposed:

$$\text{CG}\{x[n]\}(m, k) = \left| \mathcal{F}^{-1} \left\{ \log(|\text{STFT}\{x[n]\}(m, k)|^2) \right\} \right|^2, \quad (2)$$

in which \mathcal{F}^{-1} is the inverse Fourier transform. Also here, the calculation of CG for a single m is referred to as a “trace” and corresponds to a single integration interval of N samples. The running variable of the cepstrum has the dimension of seconds and has been coined “quefrequency”. The micro-Doppler periodicity expressed in hertz can be obtained by taking the inverse of the quefrequency.

The cepstrogram will prove particularly valuable in the case of long integration interval measurements on rotor or propeller-driven targets. We can use it to determine the micro-Doppler periodicity, which is related to the blade flash frequency, which in turn is related to the angular velocity of the rotor or propeller (see Fig. 3 and the Discussion). We can determine whether we deal with a single rotor or multicopter-type target (see Fig. 4 and the Discussion). In clear cases, we can even estimate the number of rotors and their individual angular velocities.

To further demonstrate the potential of the cepstrogram, we point out the natural cyclic property of the inverse Fourier transform in equation (2). This property allows for extracting the micro-Doppler periodicity even in case of under sampling. The micro-Doppler periodicity feature is sufficient to discriminate man-made objects and bio-life. Consider the following simulation of a mini-UAV with four rotors each with two blades of 12 cm length. The average rotation rate is 80 rounds per second (RPS), with 6 RPS difference between the rotors. In addition, 3 RPS variance has been added to each rotor to account for some minor steering dynamics over time. Now, let us assume an X-band radar with a sampling rate of only 3 kHz, corresponding to practical range-Doppler surveillance operation. The blind velocity in X-band is around ± 22.5 m/s, whereas the blade tip velocity is 60.3 m/s, so significant aliasing occurs. This prohibits the extraction of the overall micro-Doppler spectrum width. However, if we monitor the cepstrogram, we can still identify

the micro-Doppler periodicity, as is shown in Fig. 2. Since the extracted quefrequencies are very low, between 4.5 and 7 ms, the target can be classified as man-made.

IV. APPLICATION ON REAL MEASUREMENTS

A low-power experimental CW radar operating in X-band was used to acquire measurements on real life targets. In Fig. 3, a measurement on a small radio-controlled (RC) helicopter is shown. The micro-Doppler spectrum width is clearly visible in the long integration interval and appears quite constant. The short integration interval reveals a relative slowly rotating, even-bladed main rotor and a much faster rotating, yet shorter second rotor (the tail rotor), also even-bladed [5]. Both rotors are also visible in the cepstrogram, with the main rotor producing the strongest signal at 20.6 ms quefrequency, which corresponds to approximately 24 RPS for the two-bladed main rotor. This value is appropriate for this particular RC helicopter.

An octocopter example is shown in Fig. 4. The short integration interval in the top right panel now appears chaotic due to the superposition of eight asynchronous rotors. The long integration interval does reveal the micro-Doppler spectrum width and quite some dynamics in the separate harmonics, but the periodicity cannot be deduced from the spectrogram. The cepstrogram however shows clear quefrequency peaks between 4.5 and 6.5 ms, corresponding to rotation rates of 76.9 RPS up to 111.1 RPS considering two-bladed rotors. This range of values is appropriate for this particular octocopter. From the cepstrogram it is clear that the rotation rates of the different rotors are continuously adapted to keep the octocopter stable in the wind.

V. RELEVANT FEATURES

Suitable features provide information on target parameters and are discriminative between relevant target classes. For reliable classification under varying conditions, features should be

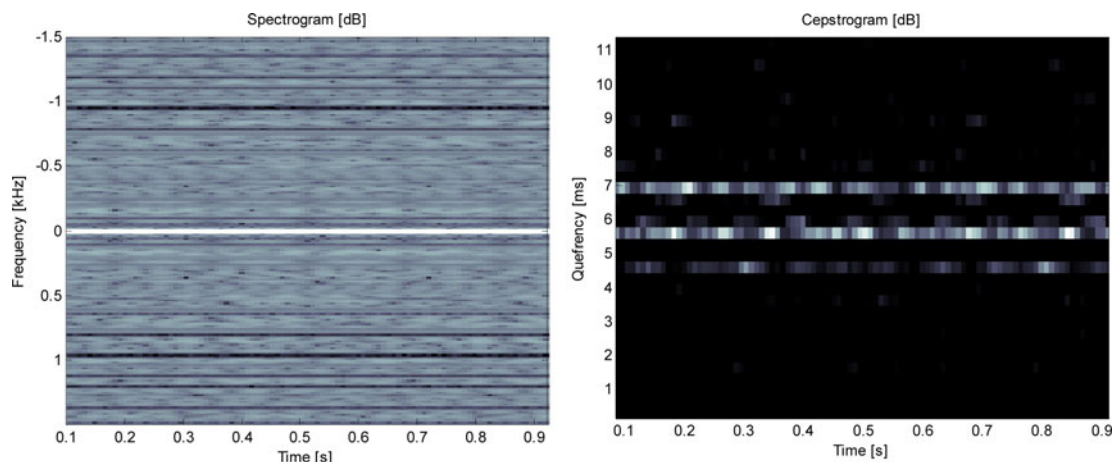


Fig. 2. Spectrogram (left) and cepstrogram (right) from a simulated stationary target with four rotors and two blades per rotor. Radar sample rate is 3 kHz.

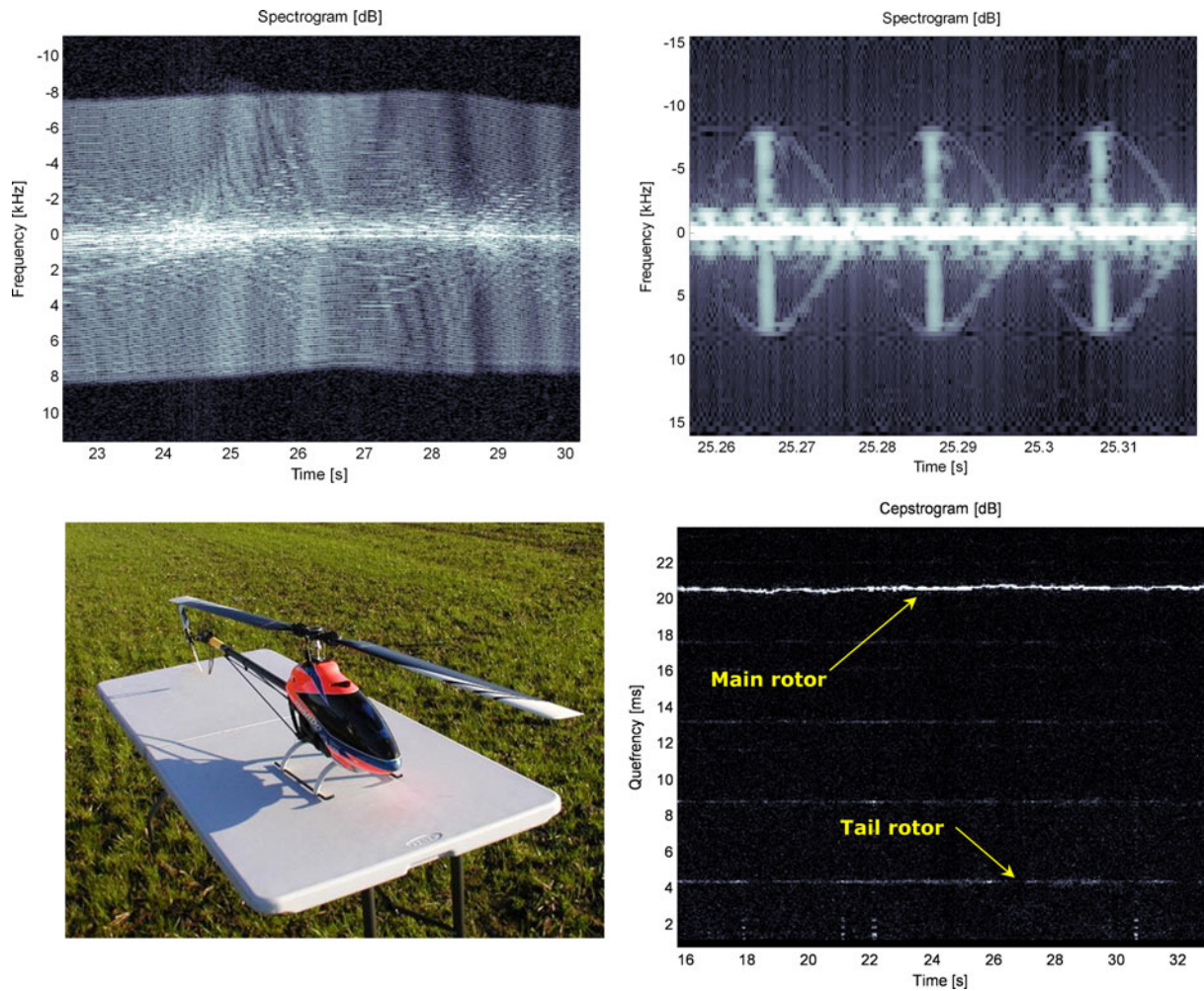


Fig. 3. Long and short integration interval spectrograms (top) of an RC helicopter shown bottom left. The cepstrogram is shown bottom right.

robust with respect to target type, radar settings, and measurement parameters, such as carrier frequency, sample rate, polarization, and aspect angle. In this section, the relevant micro-Doppler features for classification of birds and mini-UAVs are reviewed, i.e. RCS, overall target velocity, micro-Doppler periodicity and micro-Doppler spectrum width.

In general, the RCS of mini-UAVs is higher than that of birds (depending on the species). RCS is therefore a discriminative feature, but it is not a robust feature. Observed RCS levels fluctuate significantly as function of aspect angle and radar frequency. One reason is that small and medium-sized birds and mini-UAVs are in the Mie resonance region for S- and X-band radar frequencies.

Typically, the main velocity component in a spectrogram is due to the motion of a target as a whole, assuming the body or fuselage gives the strongest reflection. Velocity components due to moving parts are usually weaker. The velocity of birds and many types of mini-UAVs is in the same range, such that radial velocity is not that much discriminative. Also, radial velocity is not a robust feature in itself since it depends on direction of flight with respect to the radar.

Many target micro-motions are of periodic nature, i.e. the pendulum-like motion of a bird's wings and the rotation of rotor/propeller blades. The related spectrograms are periodic

as well. The period of a mini-UAV spectrogram is determined by the rotor rotation rate, which is generally one order of magnitude higher than that of manned helicopters. The period of a bird spectrogram is related to the wing beat cycle. The wing beat frequency of birds is between 2 and 20 beats per second, depending on the species. The periodicity of mini-UAVs can be extracted using cepstral analysis, as was discussed in Section III. In case of multiple dominant components in the spectrogram, for instance with multicopters, we can take the average periodicity (within a single trace). Furthermore, if we consider the periodicity values from multiple traces, we can calculate the variance or standard deviation on the average periodicity (from trace to trace). For multicopters we expect to find higher variance as compared with helicopters. This is because of the multiple dominant components in the cepstrogram, but also because the rotation rates of the individual rotors are continuously and rapidly adapted in order to manoeuvre and stabilize the platform. For helicopters the blade flash frequency is much more stable. Note this difference in Figs 3 and 4.

The micro-Doppler spectrum width indicates the maximum velocity of the micro-motions relative to the main velocity component. This feature can be exploited to distinguish birds from mini-UAVs. The spectrum width associated with flying birds is just several meters per second.

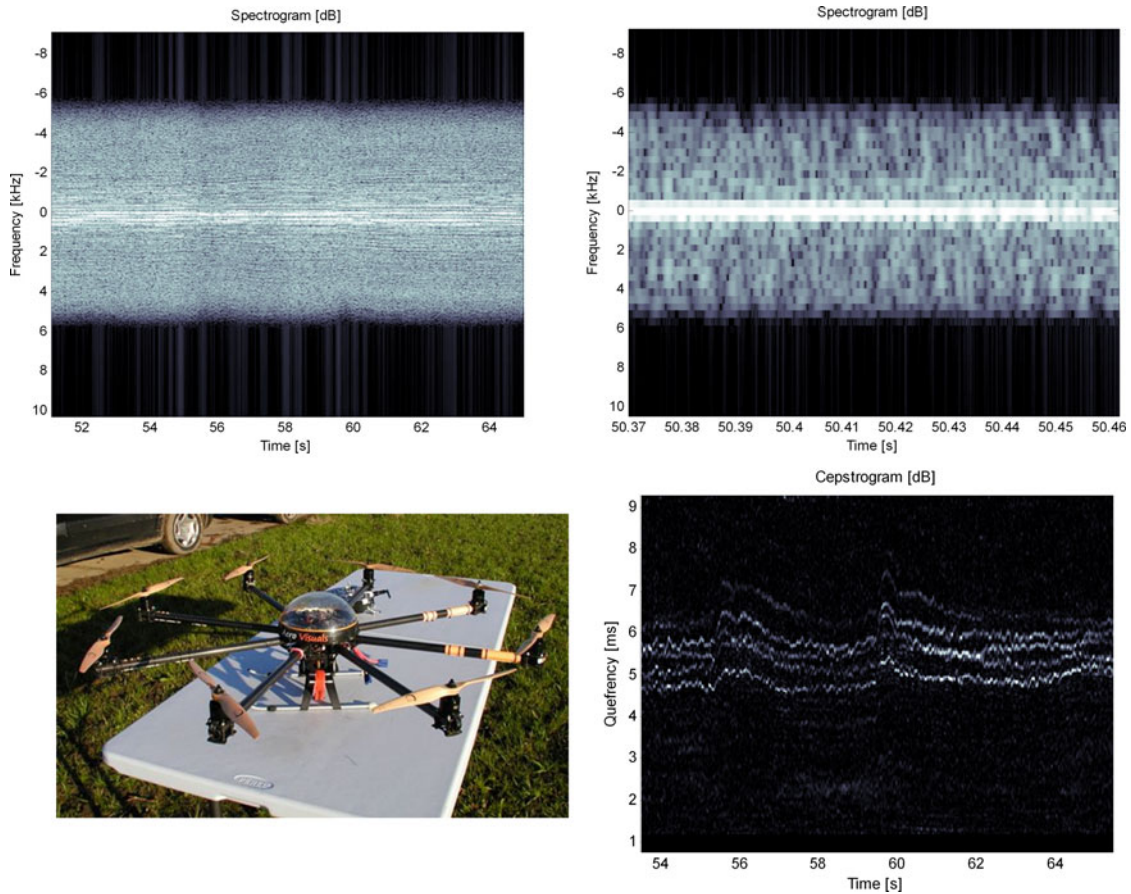


Fig. 4. Long and short integration interval spectrograms (top) of an RC octocopter shown bottom left. The cepstrogram is shown bottom right.

Typically, the velocity spread related to spinning rotors is much wider. The spectrum width feature is robust with respect to radar parameters, but it depends on the target aspect angle. High sample rates are necessary to obtain the unambiguous Doppler spectrum from mini-UAVs. Note that for range-Doppler radar, this means using specific classification waveforms with a very high PRF or SRF, as was discussed in Section II.

VI. FEATURE EXTRACTION AND CLASSIFICATION

In the remainder of this paper, we will work toward a classifier example that uses the features mentioned in Section V. All features except for *spectrum width* as we assume that we are unable to measure this feature with a radar that operates with a relatively low f_s in the spectral dimension, i.e. <10 kHz. This radar does however give us at least range and accompanying Doppler-spectrum for the unknown object. Our primary goal is to be able to make a quick distinction between a man-made object and (possible) bio-life, based on a single “scan” over the target, i.e. single time-on-target that consists of several traces. In the second step, in case of a man-made object, we would like to be able to indicate a certain subclass, e.g. whether it is a kind of helicopter or a multicopter, etc.

We try to obtain the following information for a certain number of traces M (e.g. $M = 10$), which will become our feature vector for classification:

- (1) Mean radar cross section, \overline{rcs} [m^2].
- (2) Target speed, $V_{body}(m/s)$.
- (3) Mean dominant periodicity, for each trace, $\mu_{periodicity}[Hz]$.
- (4) Standard deviation on the mean periodicity from several traces, $\sigma_{periodicity}[Hz]$.

The mean RCS for a detected target is obtained by:

$$\overline{rcs} = \frac{1}{M} \sum_{i=1}^M C_i R_i^4 \frac{S_i}{N_i}$$

S_i/N_i is the signal to (thermal) noise ratio of the main body, which is usually the strongest bin in the Doppler-spectrum outside the stationary clutter band. C_i is a radar and waveform-dependent constant, containing items such as transmit power, antenna gain, number of pulses, etc. In cases where these factors are constant for all M measurements, we may instead use $C = C_i$ for $i = 1, \dots, M$. Similarly, for a radially slow or stationary target, the range is constant $R = R_i$.

If the main body can be identified in the Doppler spectrum, then the radial velocity of the target can be extracted. Combined with the heading of the target, we may find the absolute speed V_{body} . If the heading is not known, then we may use the absolute value of the radial velocity for V_{body} instead, but then one should allow all classification models to have zero velocity as the target may fly tangentially.

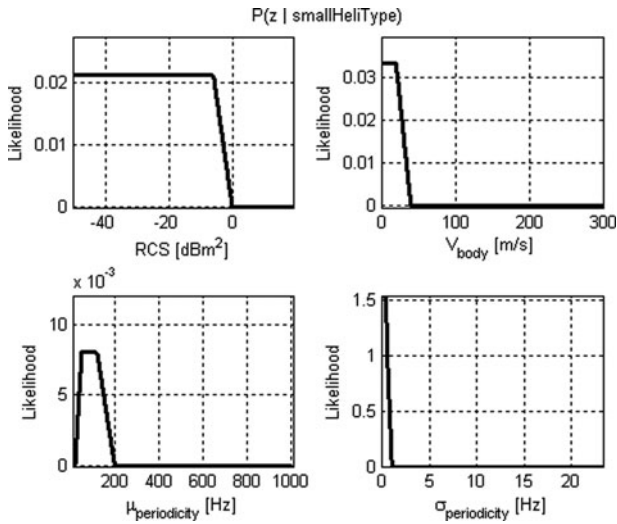


Fig. 5. Model of small model helicopters, with a single dominant rotor that gives a fairly low, yet stable blade flash frequency.

The mean periodicity is obtained from the cepstrum. Different approaches can be used, but in our case we will do the following.

- (1) Calculate the cepstrum for each trace using equation (2). We will use only the first half, i.e. $N/2$ samples, as both halves share the same content. Let q_i be the quefrency for each cell, equal to $q_i = (i - 1)/f_s$ in seconds. Let p_i be the cepstral value for cell i , with $i = 1, \dots, N/2$. In our case, we will identify the quefrencies by their index, and refrain from interpolation between cells. Note that typically $p_i \gg$ for low i as these cells cover a relative large bandwidth. For Gaussian input noise, the resulting noise distribution will appear $\propto 1/q_i$. For this reason, we will not use the first $n - 1$ samples, i.e. $Q_{all} = \{n, \dots, N/2\}$.
- (2) Apply a noise threshold, $Q_T = \{i \in Q_{all} | p_i > [c_1/q_i] + c_2\}$, where c_1 and c_2 are tuning constants to set the threshold performance.
- (3) From the threshold crossings, find the mean peaks, i.e. local maxima, $Q_{LM} = \{i \in Q_T | \exists j \in Q_T : p_i < p_j \wedge |i - j| = 1\}$.
- (4) Find the fundamental quefrencies, called "fundamentals". Often, the cepstrum shows harmonics for each

fundamental. These are called "rahmonics". We need to assess all items in Q_{LM} and decide whether they are a fundamental or a rahmonic. The following algorithm can be used for each separate trace:

- (a) *Parameters and initialization:* Let F be a variable set of fundamentals, initialized to $F := \emptyset$. Let α be a decision parameter for assessing whether two quefrencies match, set to, e.g. $\alpha = 1$. Let β be a decision parameter for assessing whether a fundamental has been found, set to, e.g. $\beta = 0.5$. Let Π be the maximum rahmonic we consider to be visible in the data, set to, e.g. $\Pi = 4$.
- (b) *Main algorithm:*
 - (i) If $Q_{LM} = \emptyset$, then stop, else, take a quefrency index $k \in Q_{LM}$ and set the current rahmonic under consideration r to $r := \Pi$.
 - (ii) If $r < 0$, then go to step i. Else, assess whether k is the r th rahmonic, in which case the fundamental $f \in Q_{all}$ would be at $f = [k/(r + 1)]$. Local maxima hits would be expected at $H = \{nf \in Q_{all} | n = 1..(r + 1)\}$. The following hits actually match the measurement $H' = \{h \in H | \exists y \in Q_{LM} : |h - y| \leq \alpha\}$.
 - (iii) If we found sufficient proof, i.e. $\#H'/(r + 1) > \beta$, then we update $F := F \cup \{f\}$ and $Q_{LM} := \{y \in Q_{LM} | \exists s \in \{1..(r + 1)\} : |s - y| \leq \alpha\}$, and go to step i, else, we assume $r := r - 1$, and go to step ii.
- (5) The fundamentals for the current trace are indexed in F . These correspond to the periodicities $1/q_k$ [Hz] with $k \in F$. The result is subject to the overall resolution of the cepstrum $1/f_s$.
- (6) Finally we take,

$$\mu_{periodicity} = \frac{\sum_{f \in F} \sum_{k=0}^{\Pi} 1/q_{(k+1)f} \cdot P_{(k+1)f}}{\#F \cdot \sum_{f \in F} \sum_{k=0}^{\Pi} P_{(k+1)f}} \quad (3)$$

The standard deviation of the periodicity $\sigma_{periodicity}$ is simply obtained by $\sigma_{periodicity} = \text{std}(\mu_{periodicity})$ with $i = 1..M$. For each radar time-on-target (i.e. the time the radar beam touches the target), consisting of M traces, of (overlapping) integration intervals of N samples, we obtain a feature vector z ,

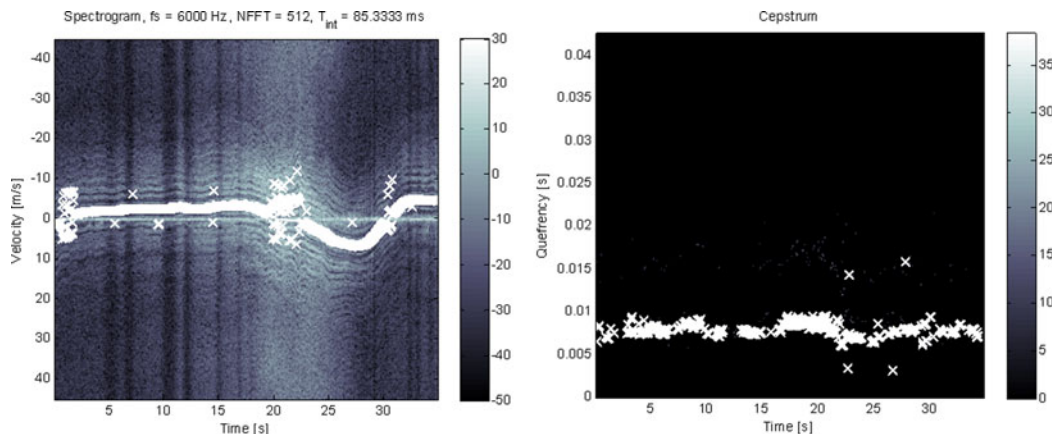


Fig. 6. Left: spectrogram of an octocopter measurement. Right: ceprogram of an octocopter measurement. "X" markers indicate the chosen fundamentals.

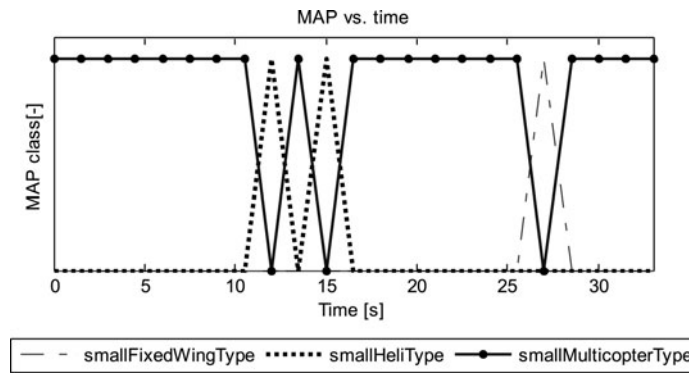


Fig. 7. Classification result of an octocopter measurement. Only classes that appear at least once are shown.

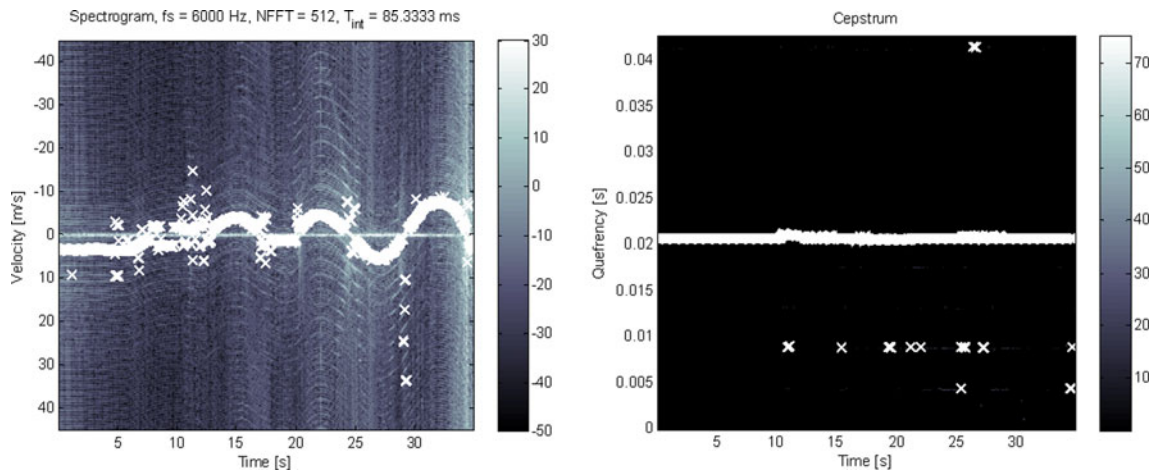


Fig. 8. Left: spectrogram of an RC helicopter measurement. Right: cepstrum of an RC helicopter measurement.

composed of, $z = [rcs, V_{body}, \mu_{periodicity}, \sigma_{periodicity}]^T$, which is then fed to the classifier.

For the sake of demonstration, we will take one of the simplest forms of classifiers, which is the MAP probability classifier, also known as the “unit cost function Bayesian”, or “minimum error rate” classifier [6]. Here, the decision function $\hat{\omega}_{MAP}(\cdot) : \mathbb{R}^N \rightarrow \Omega$, that maps the feature vector $z \in \mathbb{R}^N$ to a class $\omega_i \in \Omega$, with $i \in \{1..K\}$, is obtained by $\hat{\omega}_{MAP}(z) = \underset{\omega \in \Omega}{\operatorname{argmax}} \{p(z|\omega)P(\omega)\}$.

The conditional probability density functions $p(z|\omega_k)$ contain the discriminative information, while the priors $P(\omega)$ carry information on the composition of the entire population. Quite often however, the priors are chosen to be equal, i.e. $P(\omega) = 1/K$. Of course, in practice we could use the priors to influence our classifier, e.g. in areas with migrating birds in order to reduce the false alarm rate.

The $p(z|\omega_k)$ functions can be found using training sets and a generative learning algorithm, but it is not uncommon to just simply define them *ad hoc* using some a priori knowledge from the targets. In our case, we intend to implement the following aspects:

- (1) We are only interested in small targets that can contain either bio-life or man-made targets. Aerial target larger than, say, 0 dBm² are considered to be man-made, but need no further detailing.

- (2) Among the small aerial targets, helicopters and multicopters are more-or-less in the same velocity bracket as birds, but fixed wing aircraft can go a lot faster.
- (3) Given the chosen features, we should be able to tell apart drone helicopters, from drone fixed wing aircraft, from drone multicopters. For instance, for drone helicopters, we could argue that their blade flash frequency can be quite low compared with propeller carrying targets. And multicopters might have quite some variance on theirs, compared to helicopters and fixed wing aircraft.
- (4) In absence of clear distinctive features obtained from the cepstrum, we should conclude that no propellers or rotors are “seen” by the radar, thus the target could be anything ranging from a bird to any type of drone. Still, all bio-life will fall into this category.

Our set of classes Ω is thus chosen as follows:

$$\Omega = \{“largeManMade”, “possibleBioLife”, “smallFixedWingType”, “smallHeliType”, “smallMulticopterType”\}.$$

Instead of using a training set to shape up the target models in terms of features, we will stick to experience based, hand drawn linear likelihood curves in which we expect certain targets to appear. Because we are using features that have a physical meaning, we are able to mold the knowledge we have of our targets regarding these features, directly into the

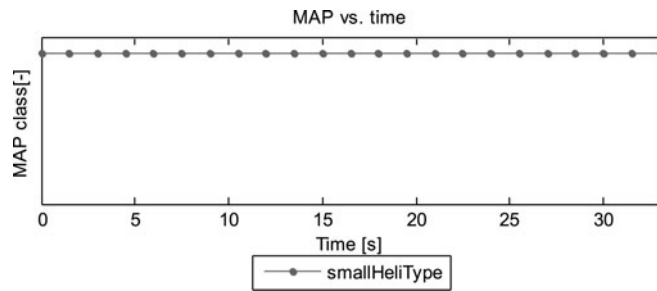


Fig. 9. Classification result of an RC helicopter measurement. Only classes that appear at least once are shown.

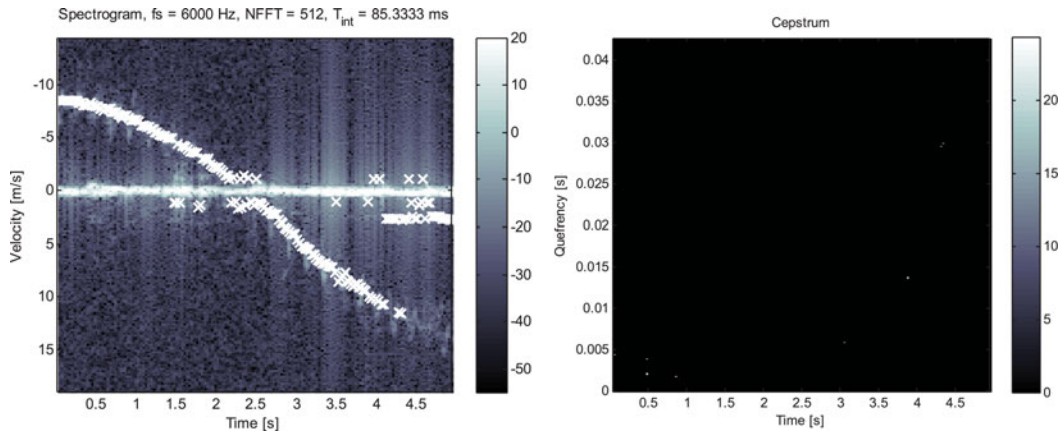


Fig. 10. Left: spectrogram of a bird measurement. Right: cepstrum of a bird measurement (no detections here)

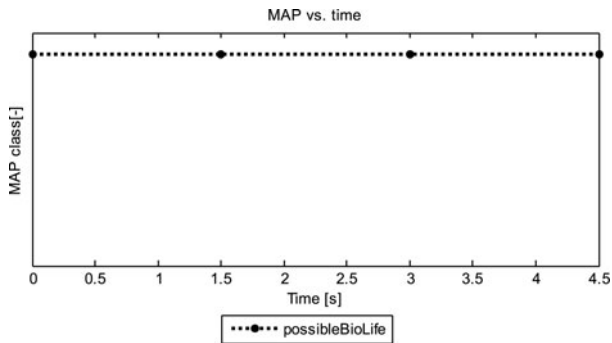


Fig. 11. Classification result of a bird measurement. Only classes that appear at least once are shown.

classifier. To illustrate this approach, the curves of the *smallHeliType* are shown in Fig. 5. From this we can, e.g. see the low $\sigma_{periodicity}$ that we would expect from an RC helicopter, whereas for a multicopter, this value is expected to be much higher.

VII. CLASSIFICATION RESULTS

Several drone and bird measurements were given as input to the classifier from Section VI. Three results are shown in Figs 6 and 7 for an octocopter measurement, Figs 8 and 9 for an RC helicopter measurement and Figs 10 and 11 for a bird measurement.

The white markers on the left panels of Figs 6, 8 and 10 indicate for each trace the bin with the strongest signal

excluding the clutter band from -1 to $+1$ m/s. This corresponds, most of the time, with the radial body velocity of the target. If the target crosses the clutter band, then wrong values are chosen, which for this particular example is not critical. The spectrograms of Figs 6 and 8 also show the long integration interval micro-Doppler signal as lines following the body signal. For the bird in Fig. 10 spectrogram wingbeat modulation is visible around the main body.

The right panels of Figs 6, 8 and 10 show the corresponding cepstrograms. In these figures, the chosen fundamentals according the algorithm in Section VI are indicated by white markers. For Fig. 6 this corresponds to an average value of 7.5 ms, or 133.3 Hz periodicity, with quite some variance. In Fig. 8, the same is shown for the helicopter: 20.6 ms (48.5 Hz), which is quite stable over time. In Fig. 10, no significant fundamental was found by the algorithm.

The classification result of the octocopter in Fig. 7 shows some confusion with “*smallHeliType*” between 11 and 16 s and with “*smallFixedWingType*” at 27 s. Most the time, however, the correct class was chosen, and at least there was never confusion with “*possibleBioLife*”. Fig. 9 shows excellent results for the “*smallHeliType*” and finally Fig. 11 scores equally great for “*possibleBioLife*”.

VIII. CONCLUSION

In this paper, we state that spectrograms and cepstrograms can be used to extract key features for automatic or visual recognition of LSS-targets versus bio-life. The long integration

interval spectrogram reveals the spectral width and body velocity. The short integration interval spectrogram shows the spectral symmetry as well as the individual rotor echoes and blade flashes. The cepstrogram shows the periodicity, and in clear cases also the number of rotors. The cepstrogram may also be particularly useful in case of lower sampling frequencies. The variance on the extracted periodicity can be used as a feature to distinguish between single, stable rotor/propeller carrying targets and multicopters such as quadcopters and octocopters.

A straightforward MAP-classifier has been used to demonstrate the potential to discriminate between possible bio-life and different types of man-made objects. Without going into performance details, this paper shows that the classifier is able to distinguish between a bird, a multicopter and a helicopter based on their micro-Doppler returns.

ACKNOWLEDGEMENTS

This study is performed in the framework of the D-RACE; the Dutch Radar Centre of Expertise, a strategic alliance of Thales Nederland B.V., and TNO. Thanks to Antonio Recinos for formatting several figures.

REFERENCES

- [1] Chen, V.: *The Micro-Doppler Effect in Radar*, Artech House, Norwood, MA, 2011.
- [2] Pennycuik, C.J.: Wingbeat frequency of birds in steady cruising flight: new data and improved predictions. *J. Exp. Biol.*, **199** (1996), 1613–1618.
- [3] Bogert, B.P.; Healy, M.J.R.; Tukey, J.W.: The Quefrency Alalysis of Time Series for Echoes: Cepstrum, Pseudo Autocovariance, Cross-Cepstrum and Saphe Cracking, *in* M. Rosenblatt (ed.), *Proc. of the Symp. on Time Series Analysis*, Wiley, New York, 1963. Chapter 15, p. 209–243.
- [4] Noll, A.M.; Schroeder, M.R.: Short-time ‘Cepstrum’ pitch detection. *in* (abstract), *J. Acoust. Soc. Am.*, **36** (5), 1030.
- [5] de Wit, J.J.M.; Harmanny, R.I.A.; Prémel-Cabic, G.: Micro-Doppler analysis of small UAV, *in* *Proc. EuRAD*, Amsterdam, The Netherlands, October 31–November 2, 2012.
- [6] van der Heijden, F.; Duin, R.P.W.; de Ridder, D.; Tax, D.M.J.: *Classification, Parameter Estimation and State Estimation*, Wiley & Sons, Chichester, UK, 2004.



Ronny Harmanny received his B.Sc. degree in Electrical Engineering in 1997 from the Hanze University of Applied Sciences, and his M.Sc. degree with honors in Computer Science in 2000 from the University of Twente. In the same year, he joined Thales Nederland B.V. as a radar system designer. He currently holds the position of Advanced Development Engineer at Thales’ Sensors department in Delft where he is involved in several innovative radar projects and studies.



Jacco de Wit received the M.Sc. and Ph.D. degrees in Electrical Engineering from Delft University of Technology, in 2000 and 2005, respectively. Since 2005 he has been employed at TNO, Department of Radar Technology, as radar systems engineer. His main research interests include advanced radar signal processing and innovative radar system concepts.



Gilles Premel-Cabic received his M.Sc. degree in Electrical Engineering in 2000 from the IRESTE Engineering School (now Ecole Polytechnique de l’Université de Nantes). He joined Thales Nederland B.V. as a radar system engineer in 2002. He currently holds the position of Advanced Development Engineer at Thales’ Sensors department in Delft.